ACS APPLIED MATERIALS & INTERFACES

Letter

www.acsami.org

Stitching Chemically Converted Graphene on Solid Surfaces by Solvent Evaporation

Yufei Wang,[†] Yuting Song,[‡,§] Satoshi Watanabe,[⊥] Suojiang Zhang,[§] Dan Li,*[,†] and Xuehua Zhang*[,‡]

[†]Department of Materials Engineering, Monash University, VIC, 3800, Australia.

[‡]Department of Chemical and Biomolecular Engineering, University of Melbourne, Melbourne, 3010, Australia

[§]Beijing Key Laboratory of Ionic Liquids Clean Processes, Key Laboratory of Green Process and Engineering, Institute of Process Engineering, Chinese Academy of Sciences, Beijing 100190, China

[⊥]Department of Chemical Engineering, Kyoto University, Nishikyo Ku, Kyoto, 6158510, Japan

Supporting Information

ABSTRACT: The suspension of chemically converted graphene (CCG) provides a cost-effective and facile approach to construct graphene-based materials. However, wrinkles and aggregates usually occur when transferring graphene from suspension to solid-state, which significantly alter the optical, electrical, and electrochemical properties of deposited graphene. Our effort is devoted to the control of the morphology of individual graphene sheet deposited on solid surfaces by the solvent evaporation. Here we have studied the effects of additional components (e.g., organic solvent and electrolyte) in the CCG suspension on the CCG morphology. It was found that the CCG sheets could be stitched together and the graphene monolayer could be flattened by the addition of appropriate additives to the CCG suspension.

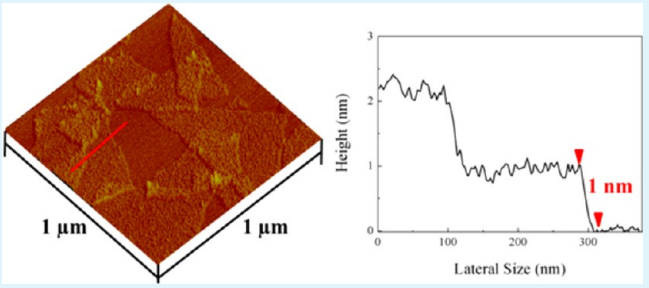

KEYWORDS: *chemically converted graphene, solvent evaporation, self-assembly, additives*

The wet-chemistry route to synthesize chemically converted graphene (CCG) by chemical reduction of graphene oxide has triggered intensive research interest since it enables cost-effective and large-scale production of individual graphene sheets as well as the ease of constructing graphene-based structures.[1−6] However, one of the challenges for processing CCG sheets is that they tend to restack, wrinkle or aggregate when they are transferred from suspension to substrates.[7−9] Because the performance of graphene-based materials is highly dependent on the arrangement of graphene sheets, a great deal of effort has been made to control the morphology of CCG sheets in the hydrated state.[10−12]

Research effort has been devoted to process graphene-based materials during the solvent evaporation in a controlled manner.[5,12,13] For example, Huang et al. synthesized crumpled graphene balls during rapid evaporation of aerosol droplets, a process that alleviated the aggregation of graphene-based materials.[14] The same protocol was also used for hybrid graphene-nanoparticle structures with energy storage applications.[15,16] Kim et al. have reported the self-assembly of graphene sheets driven by solvent evaporation process.[17] Furthermore, the latest work has demonstrated the viability of inkjet printing of graphene suspension in the fabrication of electronics.[18] We focus on the effects from the solvent evaporation on the morphology of individual graphene sheet on solid surfaces an important process for graphene patterning.[19−21]

Similar to the self-assembly behavior of nanoparticles and nanowires,[22−24] the solvent evaporation can induce self-assembly of monolayer CCG sheets on some solid surfaces.[25] It has been reported that the evaporative self-assembly is highly dependent on several factors, including surface tension of the solvent, capillary forces, particle size and shape, hydrophobicity of the particles, and the interaction potential between particles.[26−30] In particular, the self-assembled structures are influenced by the type of the substrates as well as the components of the evaporating droplet.[13,17,19−24,26−33]

In this work, we have investigated how the morphology of the CCG monolayers was altered during solvent evaporation by the additional components (organic solvent or electrolyte) in CCG aqueous suspension. The amount of additives had to be small enough to maintain dispersibility of CCG sheets, but sufficient enough to influence the various interactions during solvent evaporation process. Our results have shown that CCG sheets were assembled to connect or overlap with neighboring sheets, or to say "stitch together", in a controlled manner by the addition of appropriate components to the suspension.

Received: October 5, 2012
Accepted: November 12, 2012
Published: November 12, 2012

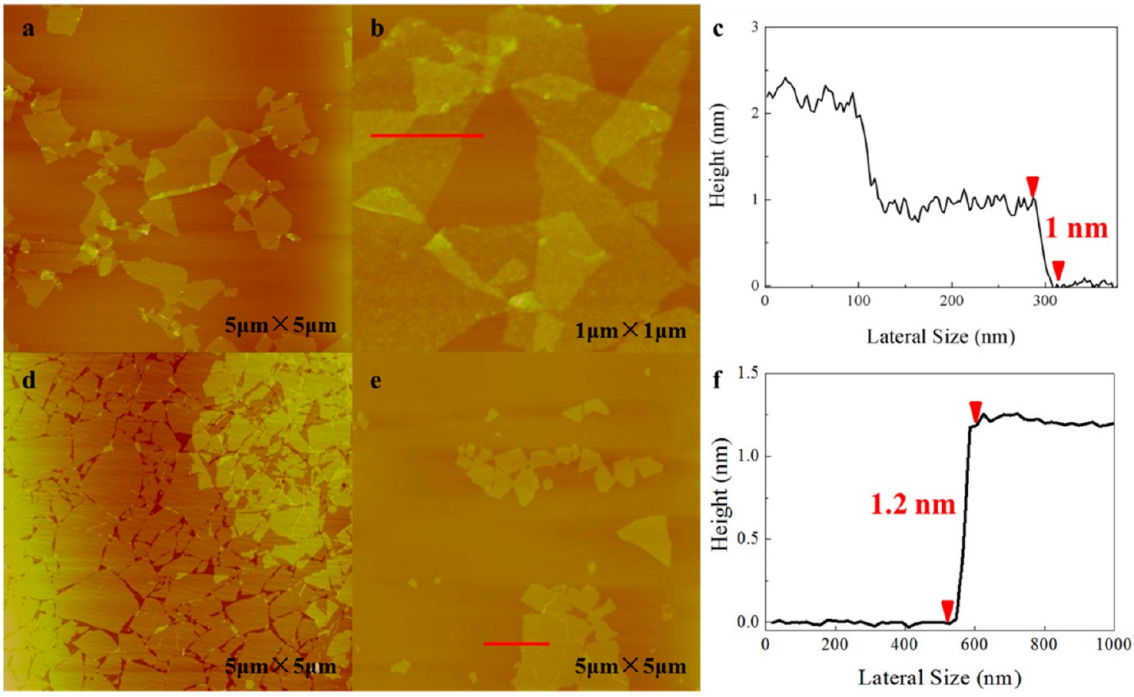

Figure 1. Morphology of CCG/GO deposited on negatively charged hydrophilic mica surface by drying a drop of CCG/GO solution containing 3 vol % ethanol. (a, b) AFM images of CCG on a mica surface; (c) cross-sectional profiles of b; (d, e) AFM images of GO on a mica surface; and (f) cross-sectional profiles of e.

Representative AFM images in Figure 1ab show the morphology of CCG monolayer on a negatively charged hydrophilic mica prepared by drop casting of CCG suspension in 3 vol % ethanol. All the CCG sheets appeared to be flat regardless of their size and geometry. No corrugations, folds or wrinkles were observed on the sheets. The average height of CCG was measured to be approximately 1 nm with the lateral dimension varying from less than 500 nm to more than 1 μm. In terms of the morphology of single-layer CCG sheets on mica surface, it was the same as those prepared without the addition of ethanol.[25,34] However, we noticed the effect of ethanol on the organization between monolayer CCG sheets on mica surface: the edge of the individual sheet overlapped obviously with the neighboring sheet. This phenomenon was in contrast to the edge-to-edge configuration of deposited CCG on mica surface without the addition of ethanol.[25] The height of the overlaid area was about 2 nm, same as two single-layer sheets. It was highly reproducible to produce such organization of flat CCG sheets with overlaid edges . The percentage of isolated CCG sheets over the area of 250 square micrometer from in 10 AFM images was found to be close to zero (Figure 3). More AFM images are provided in the Supporting Information.

As a comparison, graphene oxide (GO) suspension in 3 vol% ethanol was also deposited under the same conditions. Over a large area shown in Figure 1d, the GO sheets were closely packed to an edge-to-edge configuration and in some regions more than one layer of GO was deposited. Where there was a low number density (Figure 1e), GO sheets tended to come together rather than distribute randomly . No overlaid or folded edges were observed. It was noted that, during the packing at air−water interface in Huang's work, the GO sheets rolled up on the edge due to the strong electrostatic repulsions between neighboring sheets.[35] Here the addition of ethanol in the suspension might have mediated the electrostatic repulsion between the polar groups at the edges of GO sheets and led to the connection of GO sheets side by side.

The effect of the addition of ethanol in suspension was particularly outstanding when a positively charged surface, poly(diallyldimethylammonium chloride) coated mica surface (PDMA-mica), was used . CCG sheets were flattened and assembled to an edge-to-edge configuration (Figure 2a, b). This is in stark contrast to randomly distributed and corrugated CCG sheets on the same surface without the addition of ethanol.[25] With the addition of ethanol, less than 1% of CCG sheets were isolated from the other sheets (Figure 3). So ethanol had enabled the flattening and self-assembly of CCG on PDMA-mica surface. The CCG sheets on PDMA-mica surface appeared relatively rough, possibly because of the roughness of the underneath substrate.

CCG sheet did not assemble to an edge-to-edge configuration on another positively charged substrate, $NiCl_2$ modified mica (Ni^{2+}−mica), although most of the monolayers were flattened., There were ridges or folds observed on some sheets (Figure 2d, e). The cross-sectional profiles show an average height of about 0.8 nm for monolayer and 1.7 nm for bilayers. So the presence of ethanol did not influence the organization of CCG on Ni^{2+}−mica, in contrast to the situation on PDMA-mica surface.

On a hydrophobic surface of thiol-coated gold, the flattening of CCG sheets did not occur, but all the sheets were connected together (Figure 2g, h). Less than 2% sheets were isolated from others. This is distinctive from from the random distribution of wrinkled and corrugated CCG sheets on the same surface without ethanol in suspension.[25] Table 1 summarizes the effects of ethanol on the deposition of CCG .

The effect of another type of additive, electrolyte NaCl, was also studied. With the addition of NaCl (1 mM) to CCG suspension, the droplet evaporation created the pattern of flattened and connected CCG sheets on both mica and PDMA-

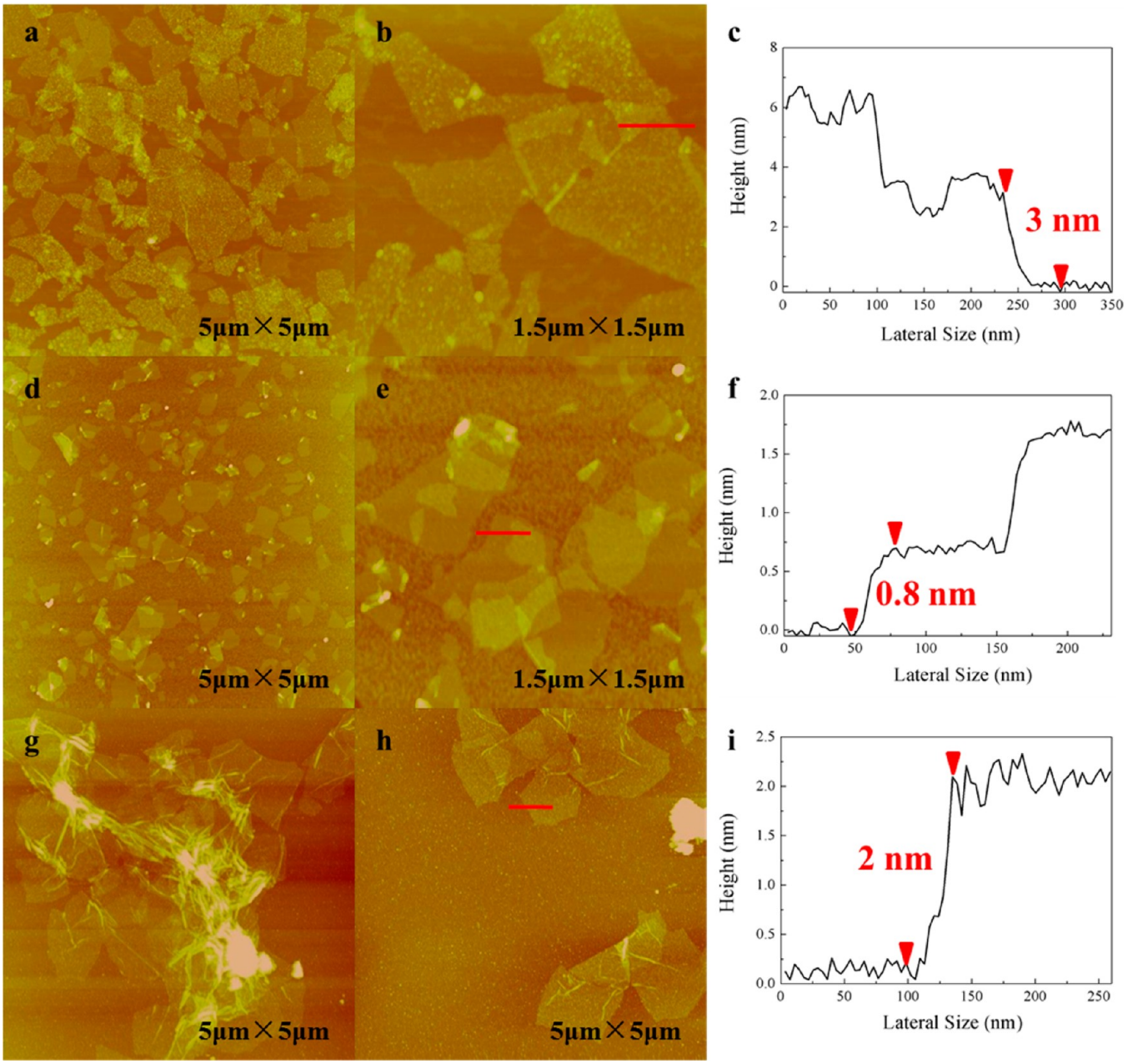

Figure 2. Morphology of CCG deposited on various types of surfaces after drying a drop of CCG solution containing 3 vol % ethanol. (a, b) AFM images on a PDMA-mica surface; (c) cross-sectional profiles of b; (d, e) AFM images on a Ni^{2+}-mica surface; (f) cross-sectional profiles of e; (g, h) AFM images on a thiol-coated gold surface; and (i) cross-sectional profiles of h.

mica (Figure 4a–f). The connection of the sheets was either by an edge-to-edge or an overlapped manner. In addition, when 1-butyl-3-methylimidazolium tetrafluoroborate ($BmImBF_4$) was used as the added electrolyte. AFM images measured an average height of monolayer CCG sheets of around 1.4 nm on mica (Figure 4i). This is higher than that of pure monolayer of CCG sheets on mica, possibly due to the adsorption of $BmImBF_4$ onto CCG sheets. The presence of $BmImBF_4$ led to flattened and connected CCG sheets, in a manner similar to the cases with the addition of ethanol or NaCl in the CCG suspension (Figure 4g, h).

Our results clearly demonstrate that the morphology of CCG depends on the substrate properties. What was puzzling is that even on both positively charged surfaces of PDMA–mica and Ni^{2+}–mica the addition of ethanol could lead to different morphologies. We attempted to gain an insight into the difference in the morphology and assembly of CCG on these two surfaces, so the drying process of the drop was monitored on these two surfaces. The snapshots of the drying drop are shown in Figure 5, and the full information is shown in Figure S9 in the Supporting Information. On PDMA–mica surface, there was no difference between the pinning duration without (Figure 5 a1—a3) or with (Figure 5 b1—b3) the addition of ethanol. The boundary was pinned on the surface for about 240 s, followed by the retraction of the liquid film. A clear and circular coffee stain ring was then left behind.

On the Ni^{2+}–mica surface, the droplet spread over an area much larger than that on PDMA-mica surface, indicating higher wettability on the former. With the addition of ethanol (Figure 5d1—d3), the boundary of the droplet started slipping over 70

dx.doi.org/10.1021/am302225y | ACS Appl. Mater. Interfaces 2012, 4, 6443–6449

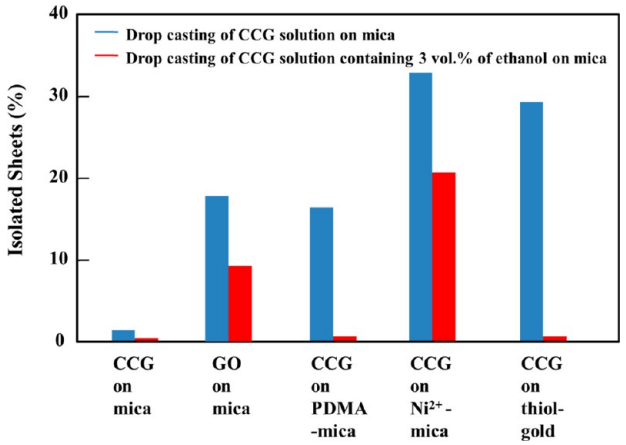

Figure 3. Comparison of the percentage of isolated CCG/GO sheets on different types of substrates between the sample prepared by drop casting of CCG solution and that of CCG solution containing 3 vol % ethanol.

s after the deposition. No clear coffee stain ring was left after solvent evaporation. The same pattern was observed without the added ethanol on Ni^{2+}-mica surface (Figure 5c1—c3): no ring was left behind. These observations support our previous hypothesis that the time of pinning had to be long enough for the self-assembly of CCG sheets to occur. The lack of assembly of CCG on Ni^{2+}—mica may be due to the higher mobility of three phase line on a relatively smooth surface.

Below we further discuss the effects of the additives from the aspects of surface tension and interactions. It has been reported experimentally that CCG sheets in water are microscopically corrugated and the amplitude of corrugation can be related to the preparation process.[10] In our previous work, the flattening and self-assembly of monolayer CCG sheets were observed on negatively charged hydrophilic substrates.[25] We proposed that the lateral capillary forces had driven the flattening and assembly of the suspended CCG at air—liquid interfaces, facilitated by the slower evaporation rate beneath the sheets and the repulsive forces between negatively charged surface and CCG sheets.[25] The addition of ethanol reduced the surface tension of the solvent from 72 mN/m (for water) to ~60 mN/m (for water containing 3 vol % ethanol).[33] This may be one of the important factors for the difference in the morphology and assembly with and without ethanol. Moreover, the presence of ethanol increased the wettability of the drop on the thiol-coated gold surface, and hence facilitated the assembly of CCG.

The surface tension of 1 mM NaCl solution is only about 0.01% less than that of water,[36] so the effect of NaCl came into play possibly through the effects on the electrostatic interactions. According to Derjaguin—Landau—Verwey—Overbeek (DLVO) theory,[37] the Debye screen length, $1/k$ with units of m^{-1}, can be expressed by eq 1

$$\kappa = (\sum_i \rho_{\infty i} e^2 z_i^2 / \in \in_0 \kappa_B T)^{1/2} \quad (1)$$

where $\rho_{\infty i}$ is the number density of ion i in the bulk solution, z is the valency of the ion, $\in$ is the relative static permittivity, $\in_0$ is the electric constant, and κ_B is the Boltzmann constant. The addition of NaCl to aqueous solution increases the number density of ions in the solution ($\rho_{\infty i}$) and screens the electrostatic force between the neighboring negatively charged CCG sheets. Especially on positively charged PDMA—mica surface, the electrostatic attractive force between CCG sheets and the substrate were also reduced with the addition of salt, enhancing the mobility of CCG sheets at the air—liquid interface for the self-assembly of the sheets.

The addition of ethanol to water reduced the relative static permittivity ($\in$) in eq 1. Hence the electrostatic interactions between neighboring CCG sheets and between the CCG sheet and the positively charged substrate were reduced, resulting in edge-to-edge configuration of GO sheets on positively charged PDMA mica surface.

Our final remark is that the height of the single graphene layer appeared to change on different substrates. As shown in the AFM images, almost all the CCG sheets are single layer graphene sheets, but with different measured heights. According to the literatures, although the theoretically estimated interlayer spacing between the graphene sheets is 0.34 nm,[38] the measured height of graphene sheets deposited on a substrate is significantly influenced by the morphology of the underneath substrate and the molecular interlayers (e.g., water containing additives in this case) between CCG and the substrate.[34,39] For example, the RMS roughness of mica, PDMA—mica, Ni^{2+}—mica and thiol—coated gold substrates were about 0.1, 1.68, 0.22, and 0.81 nm, respectively. Therefore, on smooth mica and Ni^{2+}-mica surfaces, the measured height of the CCG monolayer was about 1 nm, similar to those reported in the literature.[1,34] However, the relatively large roughness of the PDMA—mica and thiol-coated gold substrates contribute to the increased height of CCG monolayers. In addition, the adsorption of the additives (e.g., ionic liquid) on CCG can also increase the measured height of CCG sheets (Figure 4g—i).

In conclusion, we have demonstrated that in CCG deposition by solvent evaporation, a small amount of additives in the CCG suspension had a significant impact on the morphology and assembly of monolayer. Ethanol induced the overlaid arrangement of flattened sheets on negatively charged mica surface. The flattening and self-assembly behavior of sheets on positively charged surface or hydrophobic surface were achieved by the addition of ethanol or salt. Therefore, the addition of appropriate additives to the suspension is an

Table 1. Effect of Additives on the Morphology and Assembly of CCG on Solid Surfaces during Solvent Evaporation[a]

	water		3 vol % ethanol		1 mM NaCl		$BmImBF_4$	
liquid substrate	flattening	self-assembly	flattening	self-assembly	flattening	self-assembly	flattening	self-assembly
mica	√	√	√	√	√	√	√	√
PDMA-mica	×	×	√	√	√	√		
Ni^{2+}-mica	×	×	√	×				
thiol-gold	×	×	×	√				

[a](×) stands for "not observed" and (√) for "observed".

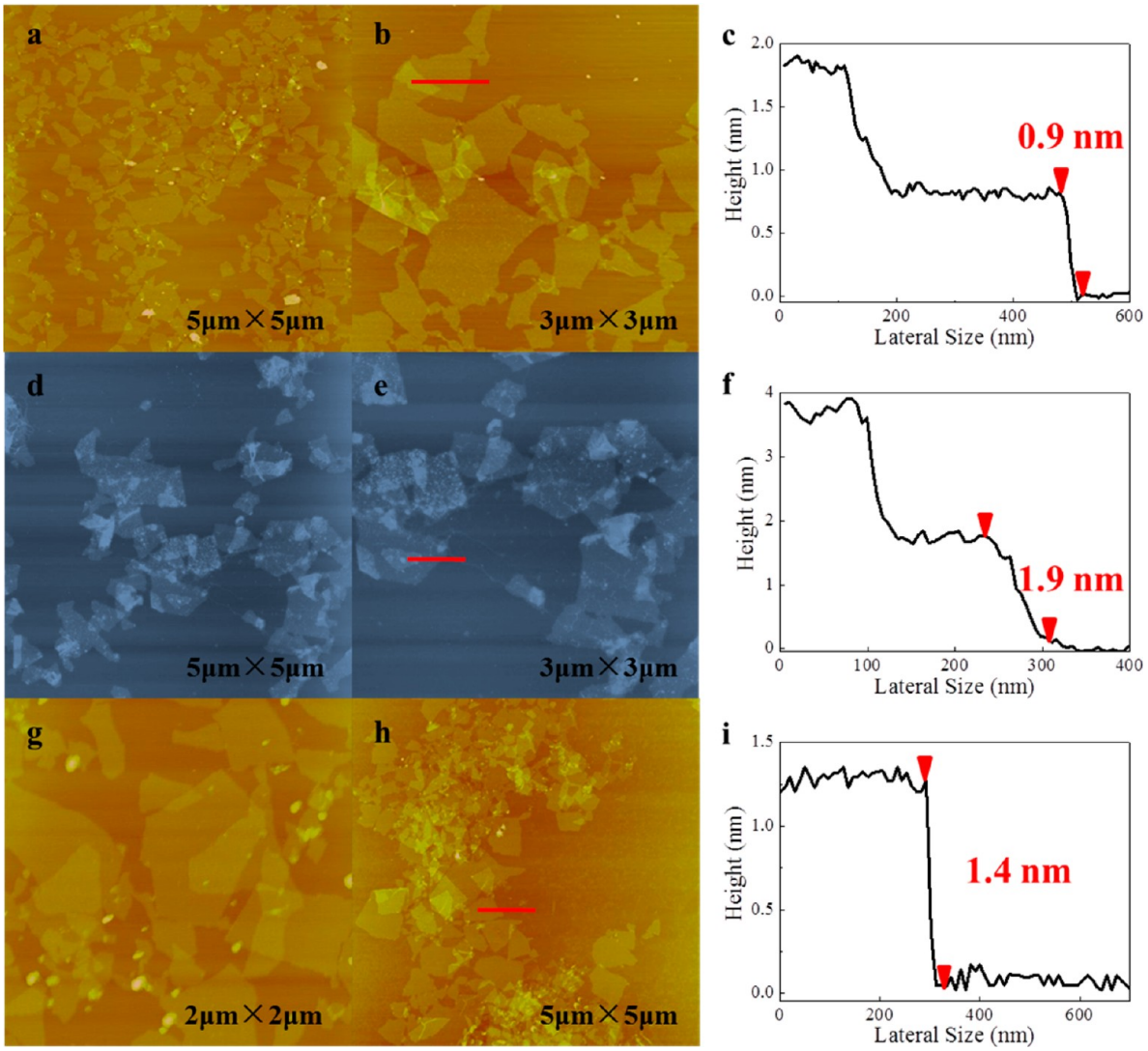

Figure 4. Effect of electrolytes on the morphology of CCG deposited on different types of surfaces: (a, b) AFM images of CCG deposited on a mica surface by drying a drop of CCG solution containing 1 mM of NaCl; (c) cross-sectional profiles of b; (d, e) AFM images CCG deposited on a PDMA-mica surface by drying a drop of CCG solution containing 1 mM of NaCl; (f) cross-sectional profiles of e; (g, h) AFM images CCG deposited on a mica surface by drying a drop of CCG solution containing $BmImBF_4$; and (i) cross-sectional profiles of h.

effective way to stitch and flatten CCG sheets deposited on a substrate by the drying process.

EXPERIMENTAL SECTION

Preparation of Graphene Oxide (GO) and Chemically Converted Graphene (CCG) Dispersions. The GO and CCG dispersions were prepared by the methods reported previously.[1] The solvent is water with less than 0.35% of ammonium which ensures stability of CCG sheets in water. The suspension was diluted by water, and CCG dispersion with concentration of 0.005 mg/mL was used for deposition CCG on solid surfaces. Typically, proper amount of additives (e.g., ethanol, NaCl, or $BmImBF_4$ aqueous solution) were added to CCG dispersion to achieve CCG dispersion containing 3 vol % ethanol, 1 mM NaCl, or 0.0025 mg/mL of $BmImBF_4$, respectively. The effect of additives with different amount was also studied, such as 2 vol % ethanol, 5 mM NaCl, and 0.005 mg/mL $BmImBF_4$, but the morphology of CCG monolayer gives a similar trend (see the Supporting Information). The measured pH values of all these dispersions were in the range of 6 to 7. The CCG suspension remained stable with the addition of the above chemicals and no aggregates were observed. This was confirmed by zeta potential measurements (ZEN3600, Malvern) (see the Supporting Information, Table S1).

Preparation of 4 Types of Substrates. Mica was freshly cleaved before use. Poly(diallyldimethylammonium chloride) coated mica (PDMA-mica) and Ni^{2+}-modified mica (Ni^{2+}-mica) surfaces were prepared by immersing the freshly cleaved mica in 1 wt % PDMA solution and 0.1 M $NiCl_2$ solution, respectively, for 30 min, followed by rinsing with Milli-Q water and drying by nitrogen stream. The thiol-coated gold surface was prepared by sputter coating of gold film on a smooth silicon surface, followed by immersing the precleaned gold substrate into 10 mM decanethiol solution in ethanol for 3 h. The gold substrate was then taken out and rinsed thoroughly with ethanol and water. The RMS roughness of mica, PDMA−mica, Ni^{2+}−mica, and thiol-coated gold substrates are about 0.1, 1.68, 0.22, and 0.81 nm, respectively, from AFM images.

Deposition of CCG-Based Solution and Characterization. A drop of CCG suspension was deposited on substrates by drop casting. The volume of the drop was 10 μL and the concentration of CCG in the suspension was 0.005 mg/mL. On the bare mica surface, since the drop tends to spread over the surface, a tiny scratch was made gently with a diamond cut to prevent the wetting film spreading outside of the surface. The substrate and the drop were then dried completely in desiccators for 1 h before imaging. The pressure in the desiccator was

dx.doi.org/10.1021/am302225y | ACS Appl. Mater. Interfaces 2012, 4, 6443−6449

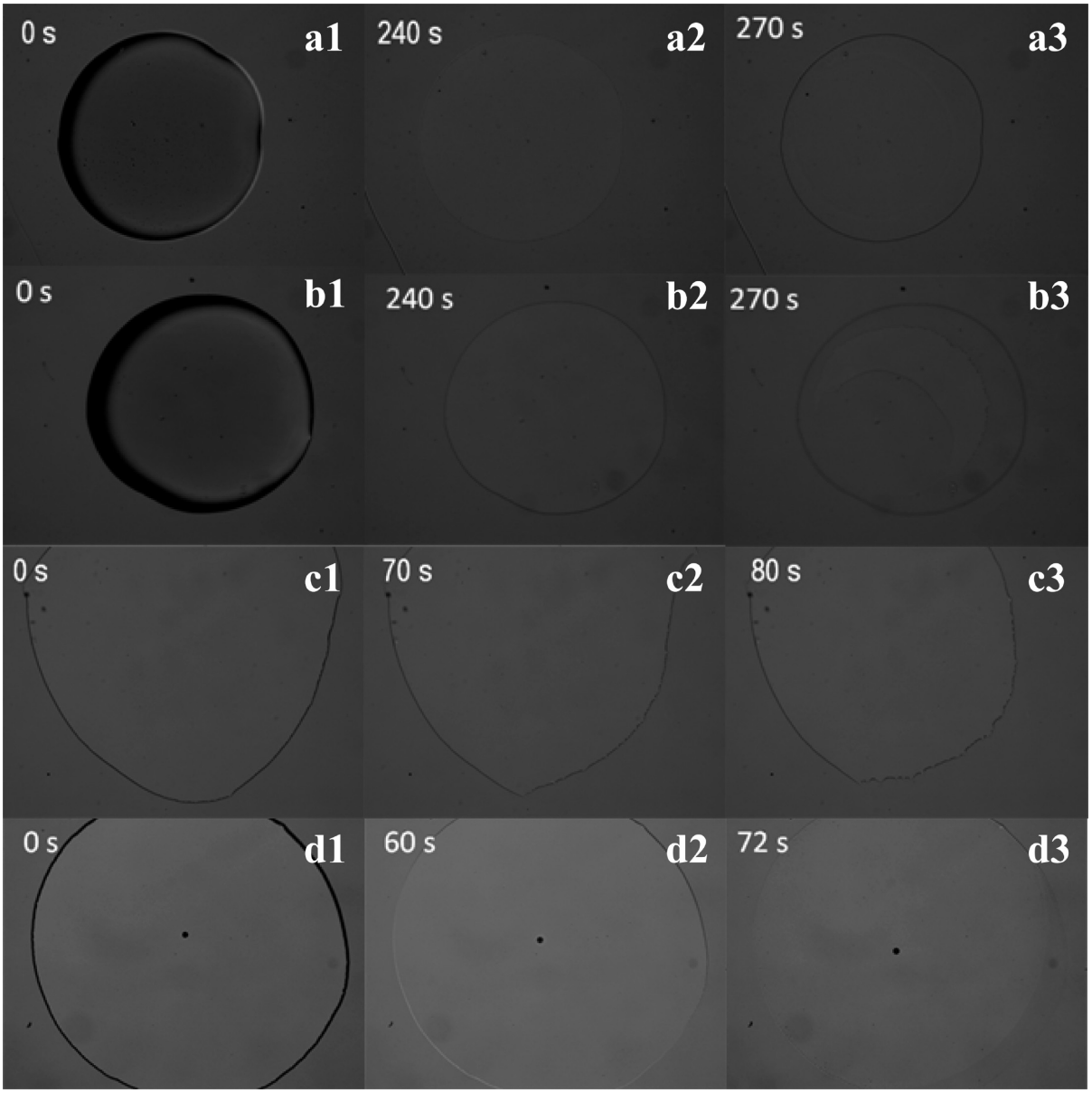

Figure 5. Snapshots of the drying process from the bottom view: the drying process of 0.2 μL drop of CCG suspension (a1−a3) without ethanol and (b1−b3) with ethanol deposited on a PDMA-mica surface; drying the same amount of CCG suspension (c1−c3) without ethanol and (d1−d3) with ethanol on a Ni^{2+}−mica surface.

kept constant through a vacuum hose at the pressure of ~20 KPa at room temperature. The concentration of the solution, the volume of the drop, and the drying conditions were the same for all the substrates.

To visualize the evaporation of the drop, we deposited 0.2 μL of the solution on the substrates of PDMA−mica and Ni^{2+}−mica surfaces. The images were taken from the bottom of the substrate by a camera (BX51, OLYMPUS, Japan) with 10 times magnification. The morphology of CCG on substrates was characterized by atomic force microscopy (Mulitmode IV, Bruker). The samples were imaged by tapping mode in air using the cantilever with the spring constant of 40 N/m (Budget Sensors Tap-300G-Al). Multiple regions near the stains were imaged for the statistic analysis.

■ ASSOCIATED CONTENT

Ⓢ Supporting Information

AFM images of CCG on different substrates and GO on mica, zeta-potential of CCG-based dispersions with additives; snapshots of drying process. This material is available free of charge via the Internet at http://pubs.acs.org.

■ AUTHOR INFORMATION

Corresponding Author

*E-mail: xuehuaz@unimelb.edu.au (X.Z.); Dan.Li2@monash.edu (D.L.).

Funding

This research was supported under Australian Research Council Discovery Projects funding scheme (DP0880152)

Notes

The authors declare no competing financial interest.

■ ACKNOWLEDGMENTS

This research was supported under Australian Research Council Discovery Projects funding scheme.

REFERENCES

(1) Li, D.; Muller, M. B.; Gilje, S.; Kaner, R. B.; Wallace, G. G. *Nat. Nanotechnol.* **2008**, *3*, 101−105.
(2) Tung, V. C.; Allen, M. J.; Yang, Y.; Kaner, R. B. *Nat. Nanotechnol.* **2009**, *4*, 25−29.
(3) Chen, H.; Muller, M. B.; Gilmore, K. J.; Wallace, G. G.; Li, D. *Adv. Mater.* **2008**, *20*, 3557−3561.
(4) Li, D.; Kaner, R. B. *Science* **2008**, *320*, 1170−1171.
(5) Yang, X.; Qiu, L.; Cheng, C.; Wu, Y.; Ma, Z.-F.; Li, D. *Angew. Chem., Int. Ed.* **2011**, *50*, 7325−7328.
(6) Xu, Y. X.; Sheng, K. X.; Li, C.; Shi, G. Q. *ACS Nano* **2010**, *4*, 4324−4330.
(7) Cote, L. J.; Kim, J.; Zhang, Z.; Sun, C.; Huang, J. X. *Soft Matter* **2010**, *6*, 6096−6101.
(8) Stoller, M. D.; Park, S. J.; Zhu, Y. W.; An, J. H.; Ruoff, R. S. *Nano Lett.* **2008**, *8*, 3498−3502.
(9) Stankovich, S.; Dikin, D. A.; Piner, R. D.; Kohlhaas, K. A.; Kleinhammes, A.; Jia, Y.; Wu, Y.; Nguyen, S. T.; Ruoff, R. S. *Carbon* **2007**, *45*, 1558−1565.
(10) Qiu, L.; Zhang, X. H.; Yang, W. R.; Wang, Y. F.; Simon, G. P.; Li, D. *Chem. Commun.* **2011**, *47*, 5810−5812.
(11) Bao, W.; Miao, F.; Chen, Z.; Zhang, H.; Jang, W.; Dames, C.; Lau, C. N. *Nat. Nanotechnol.* **2009**, *4*, 562−566.
(12) Yang, X.; Zhu, J.; Qiu, L.; Li, D. *Adv. Mater.* **2011**, *23*, 2833−2838.
(13) Chen, C. M.; Yang, Q. H.; Yang, Y. G.; Lv, W.; Wen, Y. F.; Hou, P. X.; Wang, M. Z.; Cheng, H. M. *Adv. Mater.* **2009**, *21*, 3007−3011.
(14) Luo, J. Y.; Jang, H. D.; Sun, T.; Xiao, L.; He, Z.; Katsoulidis, A. P.; Kanatzidis, M. G.; Gibson, J. M.; Huang, J. X. *ACS Nano* **2011**, *5*, 8943−8949.
(15) Xiao, L.; Damien, J.; Luo, J. Y.; Jang, H. D.; Huang, J. X.; He, Z. *J. Power Sources* **2012**, *208*, 187−192.
(16) Luo, J.; Zhao, X.; Wu, J.; Jang, H. D.; Kung, H. H.; Huang, J. *J. Phys. Chem. Lett.* **2012**, *3*, 1824−1829.
(17) Kim, T. Y.; Kwon, S. W.; Park, S. J.; Yoon, D. H.; Suh, K. S.; Yang, W. S. *Adv. Mater.* **2011**, *23*, 2734−2738.
(18) Torrisi, F.; Hasan, T.; Wu, W. P.; Sun, Z. P.; Lombardo, A.; Kulmala, T. S.; Hsieh, G. W.; Jung, S. J.; Bonaccorso, F.; Paul, P. J.; Chu, D. P.; Ferrari, A. C. *ACS Nano* **2012**, *6*, 2992−3006.
(19) Yakhno, T. A.; Sedova, O. A.; Sanin, A. G.; Pelyushenko, A. S. *Tech. Phys.* **2003**, *48*, 399−403.
(20) Craster, R. V.; Matar, O. K.; Sefiane, K. *Langmuir* **2009**, *25*, 3601−3609.
(21) Dugas, V.; Broutin, J.; Souteyrand, E. *Langmuir* **2005**, *21*, 9130−9136.
(22) Galisteo-Lopez, J. F.; Ibisate, M.; Sapienza, R.; Froufe-Perez, L. S.; Blanco, A.; Lopez, C. *Adv. Mater.* **2011**, *23*, 30−69.
(23) Masuda, Y.; Itoh, T.; Koumoto, K. *Adv. Mater.* **2005**, *17*, 841−845.
(24) Mino, Y.; Watanabe, S.; Miyahara, M. T. *Langmuir* **2011**, *27*, 5290−5295.
(25) Zhang, X.; Wang, Y.; Watanabe, S.; Uddin, M. H.; Li, D. *Soft Matter* **2011**, *7*, 8745−8748.
(26) Christy, J. R. E.; Hamamoto, Y.; Sefiane, K. *Phys. Rev. Lett.* **2011**, *106*, 205701.
(27) Dunn, G. J.; Wilson, S. K.; Duffy, B. R.; David, S.; Sefiane, K. *J. Fluid Mech.* **2009**, *623*, 329−351.
(28) Gokhale, S. J.; Plawsky, J. L.; Wayner, P. C. *Langmuir* **2005**, *21*, 8188−8197.
(29) Tay, A.; Lequeux, F.; Bendejacq, D.; Monteux, C. *Soft Matter* **2011**, *7*, 4715−4722.
(30) Truskett, V.; Stebe, K. J. *Langmuir* **2003**, *19*, 8271−8279.
(31) Deegan, R. D.; Bakajin, O.; Dupont, T. F.; Huber, G.; Nagel, S. R.; Witten, T. A. *Nature* **1997**, *389*, 827−829.
(32) Ghasemi, H.; Ward, C. A. *Phys. Rev. Lett.* **2010**, *105*, 136102.
(33) Vazquez, G.; Alvarez, E.; Navaza, J. M. *J. Chem. Eng. Data* **1995**, *40*, 611−614.
(34) Xu, K.; Cao, P. G.; Heath, J. R. *Science* **2010**, *329*, 1188−1191.
(35) Cote, L. J.; Kim, F.; Huang, J. X. *J. Am. Chem. Soc.* **2009**, *131*, 1043−1049.
(36) Jones, G.; Ray, W. A. *J. Am. Chem. Soc.* **1941**, *63*, 3262−3263.
(37) Verwey, I. J. W.; Overbeek, J. T. G. 1948.
(38) Eslami, H.; Muller-Plathe, F. *J. Phys. Chem. B* **2009**, *113*, 5568−5581.
(39) Cullen, W. G.; Yamamoto, M.; Burson, K. M.; Chen, J. H.; Jang, C.; Li, L.; Fuhrer, M. S.; Williams, E. D. *Phys. Rev. Lett.* **2010**, *105*, 215504.